

Autonomous Removal of Perspective Distortion based on Detection Results of Robotic Elevator Button Corner

MaNachuan

Department of Electronic Engineering
the Chinese University of Hong Kong
Hong Kong, China
Email: 1155135179@link.cuhk.edu.hk

Abstract—Elevator button recognition is an important function to realize the autonomous operation of elevators. However, challenging image conditions and various image distortions make it difficult to accurately recognize buttons. In this work, We propose a novel algorithm that can automatically correct perspective distortions of elevator panel images based on button corner detection results. The algorithm first leverages DeepLabv3+ model and Hough Transform method to obtain button segmentation results and button corner detection results, then utilizes pixel coordinates of standard button corners as reference features to estimate camera motions for correcting perspective distortions. The algorithm is much more robust to outliers and noise on the removal of perspective distortion than traditional geometric approaches as it only performs on a single image autonomously. 15 elevator panel images are captured from different angles of view as the dataset. The experimental results show that our approach significantly outperforms traditional geometric techniques in accuracy and robustness. Rectification results of the proposed algorithm is 77.4% better than the results of traditional geometric algorithm in average.

I. INTRODUCTION

Autonomous elevator operation appears to be a very promising solution for navigation across mobile robot floors and usually consists of three parts: button recognition, motion planning, and robot control. Button recognition is the most basic but challenging step. Its performance directly determines the success rate and robustness of the whole elevator operation system. However, current button recognition systems cannot realize autonomous operation to release human beings from tedious work. It needs human assistance or elevator panel transformation, which violates the original idea that robots are designed to be autonomous.

In recent years, various button recognition algorithms are proposed to address the problems mentioned above by using deep learning techniques [1]-[3]. And elevator button recognition algorithms usually contain two subtasks [1]: button detection and character recognition. However, due to various image conditions and distortions, the recognition accuracy is not satisfying. There are a large variety of button shapes, button sizes, elevator panel designs, and light conditions. Meanwhile, various perspective distortions and unexpected blurs make it more difficult to recognize buttons well. The

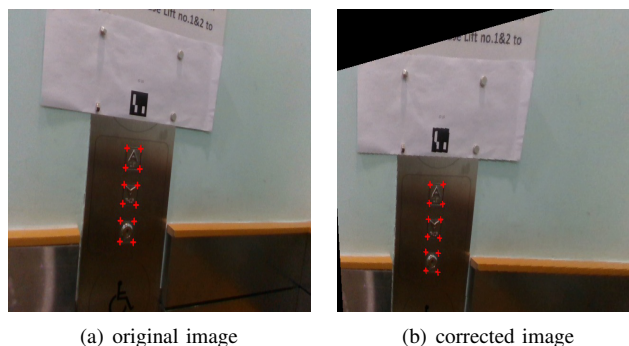


Fig. 1. A comparison between original image (left) and corrected image (right). The red crosses represent the corners of every elevator button

key idea of this work is to propose a novel algorithm that can autonomously remove such perspective distortions based on the detection results to help improve button recognition accuracy.

The corner detection approach consists of two parts. The first part is a button segmentation algorithm, which utilizes the DeepLabv3+ model to perform feature extraction and obtain button segmentation results. The second part is the corner coordinates detection algorithm. After obtaining button segmentation results, dilation and erosion procedures are utilized to reduce noise. Then Hough Transform method is applied to detect four lines of every button. Finally, pixel coordinates and the order of all button corners can be obtained as they are the intersection of detected lines.

The perspective distortion removal approach consists of four steps. The first step is to establish a standard perspective white canvas with plotting presupposed standard pixel coordinates of button corners on it. The second step is back projection. After obtaining the detection results of pixel coordinates of corners, the inverse matrix of camera intrinsic parameters is utilized to transform pixel coordinates of button corners on the normalized image plane to spatial coordinates. The third step is to estimate camera motions from images with distortion to the standard perspective white canvas. After obtaining spatial

coordinates, Rodrigues' formula is utilized and rotation degree is sampled at the interval of 0.5 of every axis to rotate spatial coordinates of the corners with distortion to obtain new spatial coordinates of them and form new spatial quadrangles. When the lines of new spatial quadrangles are parallel to the standard spatial quadrangles obtained by standard perspective button corners, we can obtain the optimal pose for camera motions. The fourth step is to form new images without distortion. After obtaining the optimal pose, each pixel of the image with distortion is transformed to new pixel coordinates by utilizing the same operation on the pixel points of corners. Through applying an inverse transformation, the perspective distortion can be removed finally. The contributions of this work are summarized as follows:

- We derive detection results of button corners by utilizing the Deeplabv3+ model and Hough Transform method.
- We propose a perspective distortion removal algorithm that can autonomously estimate distortion parameters using a single elevator panel image.

For the remaining of this work, We first introduce some related work in Sec. II, then present the corner detection process and the novel perspective distortion removal algorithm in Sec. III and Sec.IV, respectively. After that, the experimental results and discussions with traditional geometric approaches are presented in Sec. V. At the end of the work, in Sec. VI, I conclude the work and present future work.

II. RELATED WORK

A. Elevator button recognition

Before deep learning techniques are widely used in the research area of large-scale object recognition for robotics, some button recognition algorithms have already been developed by researchers. Klingbeil et al. [4] designed a pipeline that can realize button detection and character recognition, by using a grid fitting method to regress button locations after a sliding window-based object detector. Y. Lcun et al. [5] proposed a modified LeNet-5 algorithm to help implement the OCR task. The method used by Klingbeil et al. [4] achieved an accuracy of 86.2% in a test-set with 50 images. However, the size of the test-set of two methods mentioned above was too small and both of them assumed that all 50 images in the test-set were in good light conditions and could be captured without any perspective distortion. As a result, both of them cannot meet the requirement when used in real conditions. Apart from the two methods mentioned above, N. F. W. Z. Wan et al. [6] and A. A. Abdulla et al. [7] proposed some other approaches based on traditional algorithms to realize the elevator's external button recognition and visual marker-based recognition, but their abilities to handle elevator button recognition were not satisfying due to the small scale of test set images and the limited capacity of traditional algorithms.

Nowadays, there appeared an increasing number of research works regarding elevator button recognition with the wide application of deep learning techniques. Islam et al. [8] proposed a method that turned the recognition task into a classification problem and leveraged neural networks technique to

build up detection architecture. Furthermore, there emerged some publications on the topic of object detection based on a faster region-based convolutional neural network (Faster R-CNN) algorithm. For instance, S. Ren et al. [9] tried to realize real-time object detection with region proposal networks based on the Faster R-CNN algorithm. J. Dai et al. [10] modified the R-CNN algorithm and tried to realize object detection via region-based fully convolutional networks.

However, though R-CNN algorithms mentioned above worked good performance in some normalized datasets, these detection networks are restricted by the outcomes of the region proposal step. To tackle this problem, W. Liu, D et al. [10] developed a novel detection network, the Single shot multibox detector (SSD) to turn button recognition into as multi-object detection problem and can detect more objects of different sizes. Based on the work of [10], D. Zhu et al. [11] developed the R-CNN algorithm by adding a character recognition branch, converting the multi-object detection problem into two parts: binary button detection and character recognition. Compared with the Faster R-CNN based button detection architecture, this novel OCR R-CNN method showed a more accurate and robust performance on untrained elevator panel images.

In this work, we combine a more advanced semantic segmentation technique, the Deeplab model, with traditional Hough Transform method to obtain button segmentation and button corner detection results. Semantic segmentation [12-16] is one of the basic and essential topics in computer vision. It aims to classify each pixel and assign semantic labels to them in an image. Based on the Fully Convolution Neural Network [24], great improvement over systems relying on hand-crafted features [17-21] on benchmark tasks has been realized by utilizing deep convolution neural networks [22-26]. L.-C. Chen et al. [27] first proposed the Deeplabv1 model to address the task of semantic image segmentation in 2015. The Deeplabv1 model combines methods from DCNNs and probabilistic graphical models. It reaches 71.6% IOU accuracy in the test set. In 2016, the Deeplabv2 model [28] is proposed and reaches 79.7% IOU accuracy in the test set. The Deeplabv2 model can robustly perform object segmentation at multiple scales by utilizing atrous spatial pyramid pooling. After that, L.-C. Chen et al. [29] proposed the Deeplabv3 model which attained performance of 85.7% accuracy on the PASCAL VOL test set. The Deeplabv3 model adopted multiple atrous rates to design modules that could employ atrous convolution in parallel or in cascade. In 2018, L.-C. Chen et al. [30] proposed the Deeplabv3+ model which improved over previous works and reached an accuracy of 89.0%.

B. Removal of perspective distortions

In contrast to the vast literature on various elevator button recognition methods with deep learning methods, only countable publications study the removal of perspective distortions for robotic elevator button recognition. D. Zhu et al. [31] proposed an advanced method to realize automatic false-

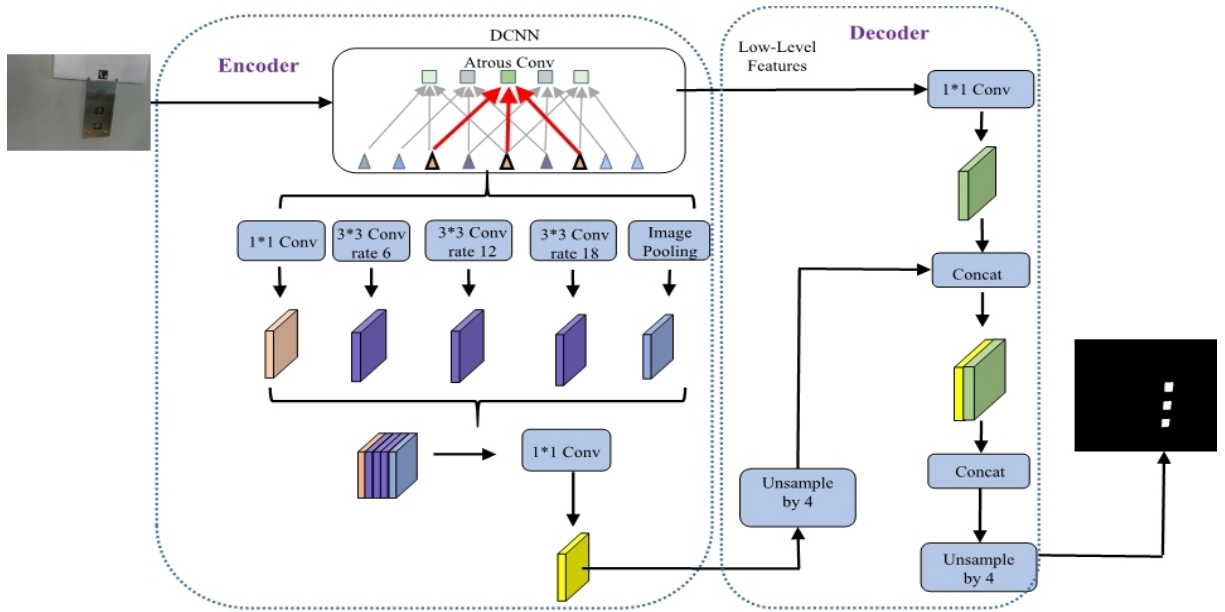


Fig. 2. DeepLabv3+ model structure.

positive canceling for indoor human detection. T. Li et al. [32] developed a hybrid 3D of pose estimation method based on camera and lidar data to help estimate transformations between the target and robot. Then Z. Min et al. [33]-[36] continued to improve the experimental results by optimizing parameters in this methodology. D. Zhu et al. [37] presented a novel algorithm based on Gaussian Mixture Model and EM algorithm, which showed a good performance in removing perspective distortions for robotic elevator button recognition autonomously in a testing elevator panel dataset of 50 images captured from different angles of view. In this work, we propose another method for perspective distortion removal by utilizing the parallelism of space quadrangle.

III. BUTTON CORNER DETECTION

A. Button Segmentation

In this work, the DeepLabv3+ model [30] is utilized to obtain segmentation results of pixels belonging to buttons. It is a typical network architecture using improved neural architecture search technology to automatically search semantic segmentation of the image. DeepLabv3+ model combines two types of neural networks together: encoder-decoder structure and spatial pyramid pooling module. By utilizing the encoder-decoder structure, we can obtain sharp object boundaries. And the spatial pyramid pooling module can capture rich contextual information by pooling features. The process of DeepLabv3+ model is shown in Fig. 2.

The input of the DeepLabv3+ model is elevator button plane images with distortion. The Mobilenet is utilized to extract features first, which is a depthwise separable convolution neural network. Based on the distorted images, Mobilenet feature extraction backbone outputs two types of features for button segmentation: low-level features and high-level

features. Then several atrous convolutions with different rates (called Atrous Spatial Pyramid Pooling) are applied to capture rich semantic information of high-level features and encode it in the output. Furthermore, the decoder module allows detailed object boundary recovery. And low-level features are combined with the output of encoder when the DeepLabv3+ model performs deconvolution decoder operation.

The output of the DeepLabv3+ model is a grayscale image with the same resolution as the input image. The value of every pixel represents which category it belongs to. For example, when this button segmentation work is applied to distorted images with three buttons, there exist four categories: 'up', 'down', 'keyhole', and 'non-button'.

B. Corner coordinates detection

After obtaining button segmentation results of distorted images, one of the button features is extracted first, and then a binary image with two categories of pixel values can be obtained, in which one category represents the button feature which we desire to extract and another represents features of the other two buttons and non-button pixels.

After that, dilation and erosion methods are utilized to reduce the noise of the binary image and smooth the edges of buttons to improve the performance of line detection. The process of erosion followed by dilation is called a closed operation. It is used to connect neighboring objects and smooth their boundaries at the same time without significantly changing their area.

Then Hough Transform method is applied to the processed image to detect four lines of the button. Hough transform is one of the basic methods to detect geometric shapes from images in the field of computer vision, image analysis, and digital image processing. It is utilized to find imperfect

instances of objects within a certain class of shapes by a voting procedure in parameter space. The transformation between two coordinate spaces is to map a curve or line with the same shape from one space to a point in another coordinate space and form a peak. Finally, after obtaining detection results of four lines of the button, we can derive pixel coordinates of button corners as they are the intersection of the detected lines. And the order of corners of every button is defined in advance to facilitate the perspective distortion removal algorithm. The order is shown as follows:

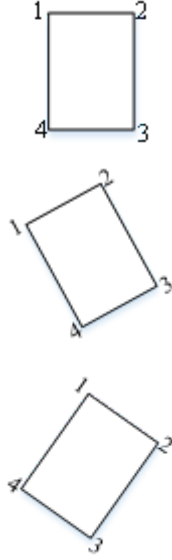


Fig. 3. The order of corners on a button.

IV. PERSPECTIVE DISTORTION REMOVAL

To begin with, we first define the notations which will be frequently used in this paper. Throughout this work, **MATRICES** are written as boldface uppercase letters and **vectors** are written as boldface lower letters. For an arbitrary matrix $\mathbf{Z} \in R^{M \times N}$ denotes the i -th column of \mathbf{Z} . The following notations are used:

- $\mathbf{C} = [\mathbf{c}_1, \dots, \mathbf{c}_N] \in R^{2 \times N}$ - the detected button corners in the image plane,
- $\hat{\mathbf{C}} = [\hat{\mathbf{c}}_1, \dots, \hat{\mathbf{c}}_N] \in R^{3 \times N}$ - the detected button corners in the normalized image plane,
- $\mathbf{U} = [\mathbf{u}_1, \dots, \mathbf{u}_N] \in R^{2 \times N}$ - the presupposed standard button corners without distortion in image plane,
- $\hat{\mathbf{U}} = [\hat{\mathbf{u}}_1, \dots, \hat{\mathbf{u}}_N] \in R^{3 \times N}$ - the presupposed standard button corners without distortion in the normalized image plane,
- $\mathbf{G} = [\mathbf{g}_1, \dots, \mathbf{g}_N] \in R^{2 \times N}$ - the rectified button corners in the image plane,
- $\hat{\mathbf{G}} = [\hat{\mathbf{g}}_1, \dots, \hat{\mathbf{g}}_N] \in R^{3 \times N}$ - the rectified button corners in the normalized image plane,

- $\mathbf{M}_{\text{int}} = \begin{bmatrix} F/s_x & 0 & o_x \\ 0 & F/s_y & o_y \\ 0 & 0 & 1 \end{bmatrix}$ - the intrinsic parameters of the camera,
- F - focal length in the meter for fixed focal length, non-zoomed camera,
- o_x, o_y - image center in pixel,
- s_x, s_y - pixel width and height in meter,
- $\mathbf{D} = [\mathbf{d}_1, \dots, \mathbf{d}_N] \in R^{3 \times N}$ - the spatial coordinate points of detected button corners,
- $\mathbf{E} = [\mathbf{e}_1, \dots, \mathbf{e}_N] \in R^{3 \times N}$ - the spatial coordinate points of standard button corners,
- $\mathbf{M} = [\mathbf{m}_1, \dots, \mathbf{m}_N] \in R^{3 \times N}$ - new spatial coordinate points of detected button corners after rotation operation,
- $\mathbf{P} = [\mathbf{p}_1, \dots, \mathbf{p}_N] \in R^{3 \times N}$ - new spatial coordinate points of detected button corners with depth equal to 1 after rotation and translation operation,
- $\mathbf{R}(\theta)$ - the matrix representation of angle-axis parameterized rotation θ ,
- \mathbf{T} - the matrix representation of translation, between detected button corners and standard button corners,
- b - the number of buttons on image,
- $\mathbf{K}_H = [\mathbf{k}_{h1}, \dots, \mathbf{k}_{hN}] \in R^{1 \times N}$ - slopes of the horizontal line of every button in space coordinate,
- $\mathbf{K}_V = [\mathbf{k}_{v1}, \dots, \mathbf{k}_{vN}] \in R^{1 \times N}$ - slopes of the vertical line of every button in space coordinate,
- $\mathbf{Cos} = [\mathbf{Cos}_1, \dots, \mathbf{Cos}_N] \in R^{1 \times N}$ - slopes of the vertical line of every button in space coordinate.

The first step is to establish a standard perspective white canvas with plotting presupposed standard pixel coordinates of the button corners \mathbf{U} on it. One demo of the standard perspective white canvas is shown in figure. 4:

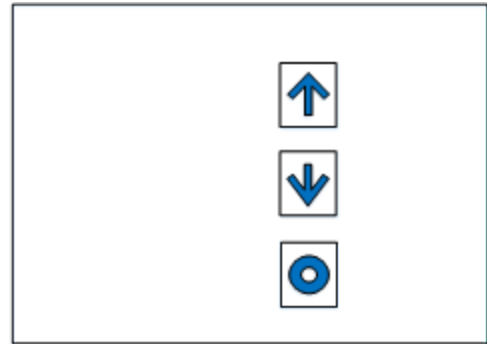


Fig. 4. One type of standard white canvas without perspective distortion.

The second step is back projection. After obtaining the detection results of the pixel coordinates of corners, the camera intrinsic parameters \mathbf{M}_{int} is utilized to realize the back-projection of pixel coordinates on normalized image plane to spatial coordinates. Pixel points in normalized image plane $\hat{\mathbf{C}}$ and $\hat{\mathbf{U}} \in R^{3 \times N}$ are obtained by adding a third row $[1 \dots 1]$ to \mathbf{C} and $\mathbf{U} \in R^{2 \times N}$.

The inverse matrix of camera intrinsic parameters is

leveraged to obtain the spatial coordinate points of button corners, and the formula is shown as follows:

$$\mathbf{D} = M_{\text{int}}^{-1} * \hat{\mathbf{C}}, \quad (1)$$

where the last row of \mathbf{D} and $\hat{\mathbf{C}}$ equals to $[1 \cdots 1]$.

Then we can obtain \mathbf{D} and \mathbf{E} from $\hat{\mathbf{C}}$ and $\hat{\mathbf{U}}$. In this work, we assume that for the standard perspective button corners without distortion, the slopes of horizontal lines equal to zero, the slopes of vertical lines equal to infinity and the cosine values of the angle between horizontal and vertical lines equal to zero. Thus for \mathbf{E} , we have:

$$\mathbf{K}_H = 1/\mathbf{K}_V = \mathbf{Cos} = [0, \cdots, 0] \in R^{1 \times N}. \quad (2)$$

The third step is to compute the rotation and translation matrix to form new spatial coordinate points of detected button corners. After obtaining spatial coordinate points \mathbf{D} , Rodriguez rotation formula is utilized to rotate spatial coordinates of the corners with distortion to obtain new spatial coordinate points of them and form new spatial quadrangles.

Rodriguez rotation formula contains three parts, including rotating θ_x against the x-axis, θ_y against the y-axis and θ_z against the z-axis, shown as follows respectively:

$$\mathbf{R}_x = \begin{bmatrix} 1 & 0 & 0 \\ 0 & \cos(\theta_x) & \sin(\theta_x) \\ 0 & -\sin(\theta_x) & \cos(\theta_x) \end{bmatrix}, \quad (3)$$

$$\mathbf{R}_y = \begin{bmatrix} \cos(\theta_y) & 0 & -\sin(\theta_y) \\ 0 & 1 & 0 \\ \sin(\theta_y) & 0 & \cos(\theta_y) \end{bmatrix}, \quad (4)$$

$$\mathbf{R}_z = \begin{bmatrix} \cos(\theta_z) & \sin(\theta_z) & 0 \\ -\sin(\theta_z) & \cos(\theta_z) & 0 \\ 0 & 0 & 1 \end{bmatrix}, \quad (5)$$

where $\theta_x, \theta_y, \theta_z$ are radian values and the relation between angle value and radian value is:

$$\text{radian value} = \frac{\text{angle value} * \pi}{180}. \quad (6)$$

Then the rotation matrix for spatial coordinate points can be obtained:

$$\mathbf{R}(\theta) = \mathbf{R}_x * \mathbf{R}_y * \mathbf{R}_z. \quad (7)$$

Finally, we can obtain new spatial coordinate points of detected button corners with depth equals to 1, and the formulas are shown as follows:

$$\begin{aligned} \mathbf{M} &= \mathbf{R}(\theta) * \mathbf{D}, \\ \mathbf{P} &= \mathbf{M} + \mathbf{T}, \\ \mathbf{P} &= \mathbf{P}/\mathbf{P}[3], \end{aligned} \quad (8)$$

where $\mathbf{P}[3]$ represents the third row of new spatial coordinate points and the translation matrix \mathbf{T} is defined as the difference value between spatial coordinate point value of the first corner in the standard perspective image and in the image needed to be rectified,

$$\mathbf{T} = \mathbf{e}_1 - \mathbf{m}_1. \quad (9)$$

The fourth step is to estimate camera motions from these images by aligning the distorted image to the standard perspective white canvas. That is to say, we desire to get the optimal rotation and translation matrix that can obtain new spatial coordinate points that make up new quadrangles in which both lines are parallel to the lines in quadrangles made up by the spatial coordinate points of the standard perspective canvas.

In this work, We sample every 0.5 degrees against each axis to obtain rotation matrix $\mathbf{R}(\theta)$ from -40 degrees to 40 degrees. There are 512,000 combinations in all.

Then three criteria are set to decide which combination can obtain the optimal rotation matrix.

The first criterion is the slopes of horizontal lines of every button in space coordinate, \mathbf{K}_H . And \mathbf{k}_{hi} of each button is defined as:

$$\mathbf{k}_{hi} = \frac{y_2 - y_1}{x_2 - x_1}, \quad (10)$$

where y_2, y_1 are the second values of the second corner spatial point and the first corner spatial point, and x_2, x_1 are the first values of the second corner spatial point and the first corner spatial point. Then we can obtain the two-norm result of \mathbf{K}_H ,

$$\|\mathbf{K}_H\|_2 = \sqrt{\sum_{i=1}^b \mathbf{k}_{hi}^2}. \quad (11)$$

When $\|\mathbf{K}_H\|_2$ is smaller, we can obtain a better result of horizontal lines of buttons.

The second criterion is slopes of vertical lines of every button in space coordinate, \mathbf{K}_V . And \mathbf{k}_{vi} of each button is defined as:

$$\mathbf{k}_{vi} = \frac{y_4 - y_1}{x_4 - x_1}, \quad (12)$$

where y_4, y_1 are the second values of the fourth corner spatial point and the first corner spatial point, and x_4, x_1 are the first values of the fourth corner spatial point and the first corner spatial point. Then we can obtain the two-norm result of \mathbf{K}_V and its reciprocal \mathbf{K}_{rV} ,

$$\begin{aligned} \|\mathbf{K}_V\|_2 &= \sqrt{\sum_{i=1}^b \mathbf{k}_{vi}^2}, \\ \mathbf{K}_{rV} &= 1 / \|\mathbf{K}_V\|_2. \end{aligned} \quad (13)$$

When \mathbf{K}_{rV} is smaller, we can obtain a better result of vertical lines of buttons.

The third criterion is cosine values of horizontal and vertical lines of every button in space coordinate, \mathbf{Cos} . The horizontal line vector, vertical line vector, and \mathbf{cos}_i of each button are shown as follows:

$$\begin{aligned} h &= (x_2 - x_1, y_2 - y_1, z_2 - z_1), \\ v &= (x_4 - x_1, y_4 - y_1, z_4 - z_1), \\ \mathbf{cos}_i &= \frac{h \bullet v}{\|h\|_2 \bullet \|v\|_2}, \end{aligned} \quad (14)$$

where (x_1, y_1, z_1) is the spatial coordinate point of the first

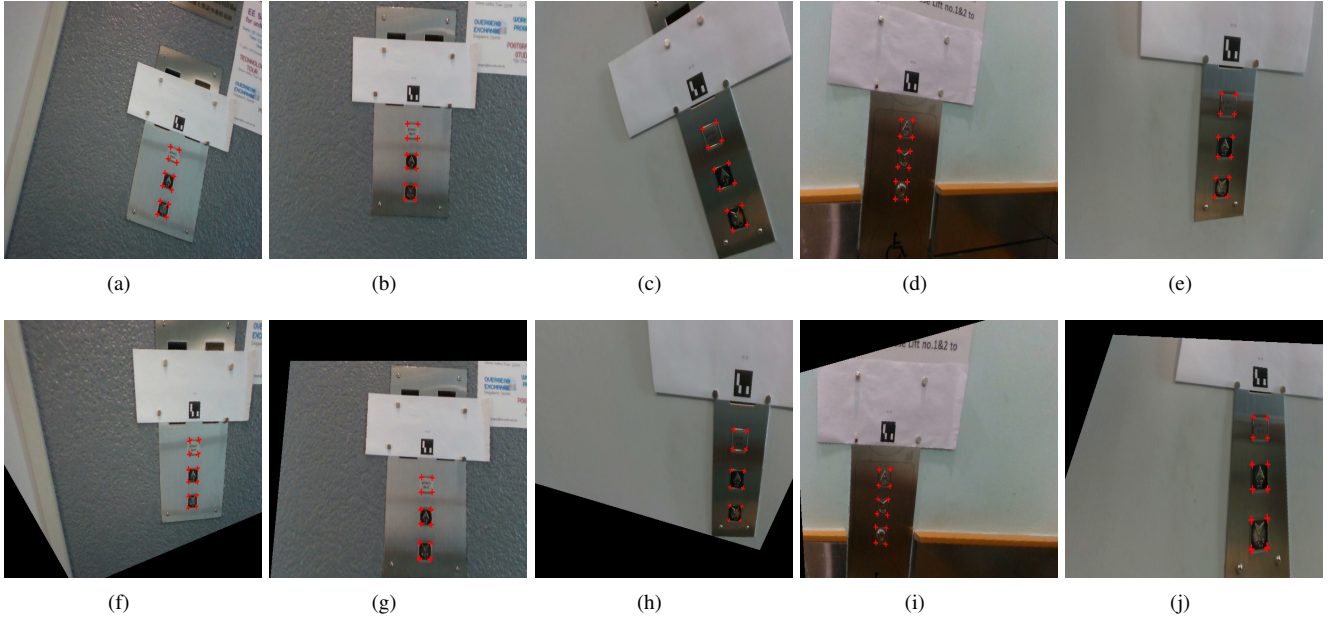


Fig. 5. Demonstrations of perspective distortion removal. (a)(b)(c)(d)(e) represent original elevator button panel images. (f)(g)(h)(i)(j) represent the corrected elevator button panel images respectively.

corner, (x_2, y_2, z_2) is the spatial coordinate point of the second corner, and (x_4, y_4, z_4) is spatial coordinate point of the fourth corner. Then we can obtain the two-norm result of \mathbf{Cos} ,

$$\|\mathbf{Cos}\|_2 = \sqrt{\sum_{i=1}^b \mathbf{cos}_i^2}. \quad (15)$$

When $\|\mathbf{Cos}\|_2$ is smaller, we can obtain a better perpendicular result of horizontal and vertical lines of buttons.

To combine the three criteria, they are normalized for all rotation matrix combination conditions,

$$\hat{\mathbf{K}}_H = \frac{\|\mathbf{K}_H\|_2 - (\|\mathbf{K}_H\|_2)_{\min}}{(\|\mathbf{K}_H\|_2)_{\max} - (\|\mathbf{K}_H\|_2)_{\min}}, \quad (16)$$

$$\hat{\mathbf{K}}_{rV} = \frac{\|\mathbf{K}_{rV}\|_2 - (\|\mathbf{K}_{rV}\|_2)_{\min}}{(\|\mathbf{K}_{rV}\|_2)_{\max} - (\|\mathbf{K}_{rV}\|_2)_{\min}}, \quad (17)$$

$$\hat{\mathbf{Cos}} = \frac{\|\mathbf{Cos}\|_2 - (\|\mathbf{Cos}\|_2)_{\min}}{(\|\mathbf{Cos}\|_2)_{\max} - (\|\mathbf{Cos}\|_2)_{\min}}. \quad (18)$$

Then the final criterion is shown as follows:

$$Final\ Criterion = \hat{\mathbf{K}}_H + \hat{\mathbf{K}}_{rV} + \hat{\mathbf{Cos}}. \quad (19)$$

When Final Criterion is smallest, we can obtain the optimal rotation and translation matrix that can transform spatial coordinate points of detected button corners to the ideal spatial coordinate points of standard perspective button corners without distortion.

The fifth step is to form new images without distortion. After obtaining the optimal pose, each pixel of the image with distortion is transformed to new pixel coordinates by utilizing

the same operation on the pixel of corners.

The same type of pixel points is generated as distorted images and they are set in the normalized image plane $\in R^{3 \times N}$ by adding a third row $[1 \cdots 1]$. Then as the formula (1) shows, the inverse matrix of camera intrinsic parameters is leveraged to obtain spatial coordinate points of all pixel points.

After that, new spatial coordinate points of all pixel points with depth equal to 1 can be obtained by utilizing the formulas (8), where the optimal pose of the optimal rotation and translation matrix has been obtained by the operation for button corners before.

When new spatial coordinate points of all pixels have been obtained, we can utilize camera intrinsic parameters to do projection and get new pixel points in the normalized plane,

$$\hat{\mathbf{G}} = \mathbf{M}_{\text{int}} * \mathbf{P}. \quad (20)$$

Then by taking the first and second rows, we can obtain pixel coordinates of the rectified button corners in the image plane.

Finally, through applying an inverse transformation between the same type of a blank image and the distorted image, we can obtain a new image where the perspective distortion has been removed.

V. EXPERIMENTS

In this section, the DeepLabv3+ model has experimented on a large-scale test dataset containing high-quality pixel-level annotations of 2000 elevator button images. The experimental results show that the DeepLabv3+ model sets good performance. Then we collect a dataset with 15 images from 3 different elevators to verify the proposed algorithm and all the samples are captured from different angles of views containing severe perspective distortions. Some demonstrations of the

TABLE I

COMPARISON OF RESULTS OF DISTORTION REMOVAL ALGORITHMS. IN EACH GROUP, THE FIRST ROW PRESENTS THE IMAGE NUMBER, THE SECOND AND THIRD ROW PRESENT THE RESULT OF EQ. (15) ON RECTIFIED IMAGES RESPECTIVELY. AND WHEN THE RESULT VALUE IS SMALLER, THE RECTIFICATION RESULT IS BETTER. IN THE EXPERIMENT, RECTIFICATION RESULTS OF THE PROPOSED ALGORITHM IS 77.4% BETTER THAN THE RESULTS OF TRADITIONAL GEOMETRIC ALGORITHM IN AVERAGE.

No.1	I-10	I-20	I-30	I-40	I-50	Average	Improved rate
The proposed algorithm	0.036	0.0423	0.0498	0.0068	0.0237	0.0317	85.30%
Traditional algorithm	0.2694	0.2431	0.2423	0.1404	0.1839	0.2158	
No.2	I-160	I-170	I-180	I-190	I-200	Average	Improved rate
The proposed algorithm	0.0034	0.0262	0.0026	0.0038	0.0159	0.0104	92.30%
Traditional algorithm	0.0893	0.1062	0.1309	0.1735	0.1776	0.1355	
No.3	I-850	I-860	I-870	I-880	I-890	Average	Improved rate
The proposed algorithm	0.0482	0.07	0.0967	0.0999	0.0737	0.0777	54.60%
Traditional algorithm	0.1763	0.1758	0.1908	0.1668	0.1467	0.1713	
Average Improved rate							77.40%

original and rectified images are presented in Fig. 5. In all experiments, the camera intrinsic parameter matrix is:

To measure the accuracy and effectiveness of the proposed distortion removal algorithm, we apply the proposed algorithm and the traditional geometric algorithm to the dataset and compare the distortion removal results of them. The value of Eq. (15) is utilized for measurement, which indicates the two-norm value of cosine values between horizontal and vertical lines of all buttons in space coordinate. When the value of Eq. (15) is smaller, the rectification result is better.

The traditional geometric algorithm We utilized in my experiments is proposed by Krishnendu Chaudhury [38]. The key idea of this traditional geometric algorithm is to take the image closer to the front-parallel view by performing an affine rectification on the image that restores the parallelism of lines parallel in the front-parallel image view. It is based on RANSAC (Random Sample Consensus) approach utilizing vanishing points.

The detailed experimental comparison results are listed in Table. I. As we can see from Table. I, the proposed algorithm achieves higher accuracy on all the three groups of images. Rectification results of the proposed algorithm is 77.4% better than the results of traditional geometric algorithm in average, which strongly varies the effectiveness of the proposed algorithm. According to Fig. 5, we can see that even the image sample has very severe perspective distortion, the proposed algorithm can also perform good rectification performance.

VI. CONCLUSION

In this work, We present a novel algorithm for autonomously removing perspective distortions on a single image based on the detected results of button corners obtained by leveraging the DeepLabv3+ model and Hough Transform method. The proposed algorithm takes as input the pixel coordinate points of button corners, then conducts pose estimation procedures in space coordinate and obtains the optimal pose which can take the image closest to the front-parallel view and finally outputs the corrected images, which can help improve the accuracy of character recognition. The comparison

results between the proposed algorithm and the traditional geometric algorithm prove the effectiveness and accuracy of the proposed algorithm. In the experiment, rectification results of the proposed algorithm is 77.4% better than the results of traditional geometric algorithm in average. Currently, the algorithm can only handle elevator panel images that contain several rectangle buttons. For elevator panel images that contain circle buttons, as a circle has no slopes, the algorithm cannot be applied to. In the next step, We will try to develop a novel algorithm for autonomously removing perspective distortions on elevator images that contain round buttons by utilizing Hough Transform theory to calculate the coordinate of the circle button's center and radius value. We will also collect a larger dataset to verify the robustness of the algorithm, based on which further improvement will be made.

ACKNOWLEDGMENT

This project is partially supported by the Hong Kong RGC GRF grants #14200618 and Shenzhen Science and Technology Innovation projects c.02.17.00601 awarded to Max Q.-H. Meng.

REFERENCES

- [1] D. Zhu, T. Li, D. Ho, T. Zhou, and M. Q. Meng, "A novel ocr-rcnn for elevator button recognition," in 2018 IEEE/RSJ International Conference on Intelligent Robots and Systems (IROS). IEEE, 2018, pp. 3626–3631.
- [2] Z. Dong, D. Zhu, and M. Q.-H. Meng, "An autonomous elevator button recognition system based on convolutional neural networks," in Robotics and Biomimetics (ROBIO), 2017 IEEE International Conference on. IEEE, 2017, pp. 2533–2539.
- [3] J. Liu and Y. Tian, "Recognizing elevator buttons and labels for blind navigation," in 2017 IEEE 7th Annual International Conference on CYBER Technology in Automation, Control, and Intelligent Systems (CYBER). IEEE, 2017, pp. 1236–1240.
- [4] E. Klingbeil, B. Carpenter, O. Russakovsky, and A. Y. Ng, "Autonomous operation of novel elevators for robot navigation," in IEEE International Conference on Robotics and Automation, 2010, pp. 751–758.
- [5] Y. Lcun, L. Bottou, Y. Bengio, and P. Haffner, "Gradient-based learning applied to document recognition," Proceedings of the IEEE, vol. 86, no. 11, pp. 2278–2324, 1998.
- [6] N. F. W. Z. Wan, M. R. Daud, S. Razali, and M. F. Abas, "Elevators external button recognition and detection for vision-based system," Proceeding of the Electrical Engineering Computer Science & Informatics, 2014.

- [7] A. A. Abdulla, H. Liu, N. Stoll, and K. Thurow, "A robust method for elevator operation in semi-outdoor environment for mobile robot transportation system in life science laboratories," in IEEE Jubilee International Conference on Intelligent Engineering Systems, 2016.
- [8] K. T. Islam, G. Mujtaba, R. G. Raj, and H. F. Nweke, "Elevator button and floor number recognition through hybrid image classification approach for navigation of service robot in buildings," in International Conference on Engineering Technology and Technopreneurship, 2017, pp. 1–4.
- [9] S. Ren, K. He, R. Girshick, and J. Sun, "Faster r-cnn: towards realtime object detection with region proposal networks," in International Conference on Neural Information Processing Systems, 2015, pp. 91–99.
- [10] J. Dai, Y. Li, K. He, and J. Sun, "R-fcn: Object detection via regionbased fully convolutional networks," 2016.
- [11] D. Zhu, T. Li, D. Ho, T. Zhou, and M. Q. Meng, "A novel ocr-rcnn for elevator button recognition," in 2018 IEEE/RSJ International Conference on Intelligent Robots and Systems (IROS). IEEE, 2018, pp. 3626–3631.
- [12] Everingham, M., Eslami, S.M.A., Gool, L.V., Williams, C.K.L., Winn, J., Zisserman, A.: The pascal visual object classes challenge a retrospective. IJCV (2014).
- [13] Mottaghi, R., Chen, X., Liu, X., Cho, N.G., Lee, S.W., Fidler, S., Urtasun, R., Yuille, A.: The role of context for object detection and semantic segmentation in the wild. In: CVPR. (2014)
- [14] Cordts, M., Omran, M., Ramos, S., Rehfeld, T., Enzweiler, M., Benenson, R., Franke, U., Roth, S., Schiele, B.: The cityscapes dataset for semantic urban scene understanding. In: CVPR. (2016)
- [15] Zhou, B., Zhao, H., Puig, X., Fidler, S., Barriuso, A., Torralla, A.: Scene parsing through ade20k dataset. In: CVPR. (2017)
- [16] Caesar, H., Uijlings, J., Ferrari, V.: COCO-Stuff: Thing and stuff classes in context. In: CVPR. (2018)
- [17] He, X., Zemel, R.S., Carreira-Perpindn, M.: Multiscale conditional random fields for image labeling. In: CVPR. (2004)
- [18] Shotton, J., Winn, J., Rother, C., Criminisi, A.: Textonboost for image understanding: Multi-class object recognition and segmentation by jointly modeling texture, layout, and context. IJCV (2009)
- [19] Kohli, P., Torr, P.H., et al.: Robust higher order potentials for enforcing label consistency. IJCV 82(3) (2009) 302–324.
- [20] Ladicky, L., Russell, C., Kohli, P., Torr, P.H.: Associative hierarchical crfs for object class image segmentation. In: ICCV. (2009)
- [21] Gould, S., Fulton, R., Koller, D.: Decomposing a scene into geometric and semantically consistent regions. In: ICCV. (2009)
- [22] Yao, J., Fidler, S., Urtasun, R.: Describing the scene as a whole: Joint object detection, scene classification and semantic segmentation. In: CVPR. (2012)
- [23] LeCun, Y., Bottou, L., Bengio, Y., Haffner, P.: Gradient-based learning applied to document recognition. In: Proc. IEEE. (1998)
- [24] Krizhevsky, A., Sutskever, I., Hinton, G.E.: Imagenet classification with deep convolutional neural networks. In: NIPS. (2012)
- [25] Simonyan, K., Zisserman, A.: Very deep convolutional networks for large-scale image recognition. In: ICLR. (2015)
- [26] Szegedy, C., Liu, W., Jia, Y., Sermanet, P., Reed, S., Anguelov, D., Erhan, D., Vanhoucke, V., Rabinovich, A.: Going deeper with convolutions. In: CVPR. (2015)
- [27] L.-C. Chen, G. Papandreou, I. Kokkinos, K. Murphy, and A. L. Yuille, "Semantic image segmentation with deep convolutional nets and fully connected crfs," in ICLR, 2015.
- [28] L.-C. Chen, G. Papandreou, I. Kokkinos, K. Murphy, and A. L. Yuille. Deeplab: Semantic image segmentation with deep convolutional nets, atrous convolution, and fully connected crfs. arXiv:1606.00915, 2016.
- [29] Chen, L.C., Papandreou, G., Schroff, F., Adam, H.: Rethinking atrous convolution for semantic image segmentation. arXiv:1706.05587 (2017)
- [30] Chen, L.C., Papandreou, G., Schroff, F., Adam, H.: Encoder-Decoder with Atrous Separable Convolution for Semantic Image Segmentation. arXiv:1802.02611v3 (2018)
- [31] D. Zhu and M. Q. Meng, "Automatic false positive canceling for indoor human detection," in 2016 IEEE International Conference on Information and Automation (ICIA), Aug 2016, pp. 381–384.
- [32] T. Li, D. Zhu, and M. Q. Meng, "A hybrid 3dof pose estimation method based on camera and lidar data," in 2017 IEEE International Conference on Robotics and Biomimetics (ROBIO), Dec 2017, pp. 361–366.
- [33] Z. Min, J. Wang, S. Song, and M. Q.-H. Meng, "Robust generalized point cloud registration with expectation maximization conlintering anisotropic positional uncertainties," in 2018 IEEE/RSJ International Conference on Intelligent Robots and Systems (IROS). IEEE, 2018, pp. 1290–1297.
- [34] Z. Min, J. Wang, and M. Q. Meng, "Robust generalized point cloud registration with orientational data based on expectation maximization," IEEE Transactions on Automation Science and Engineering, pp. 1–15, 2019.
- [35] Z. Min, J. Wang, and M. Q.-H. Meng, "Joint rigid registration of multiple generalized point sets with hybrid mixture models," IEEE Transactions on Automation Science and Engineering, 2019.
- [36] Z. Min, D. Zhu, and M. Q.-H. Meng, "Accuracy assessment of an ocular motion capture system for surgical tool tip tracking using pivot calibration," in 2016 IEEE International Conference on Information and Automation (ICIA). IEEE, 2016, pp. 1630–1634.
- [37] D.Zhu, J.Liu, N.Ma, and M. Q.-H. Meng, "Autonomous Removal of Perspective Distortion for Robotic Elevator Button Recognition," in 2019 IEEE International Conference on Robotics and Biomimetics (ROBIO), Dec 2019.
- [38] Chaudhury, Krishnendu, Stephen DiVerdi, and Sergey Ioffe. "Auto-rectification of user photos." 2014 IEEE International Conference on Image Processing (ICIP). IEEE, 2014.